

Properties and preparation of olefin block copolymer/thermoplastic polyurethane blends

Wen-Chih Chen,¹ Sun-Mou Lai,² Zong-Ching Liao³

¹Department of Chemical Engineering, Chinese Culture University, Taipei 111, Taiwan, ROC

²Department of Chemical and Materials Engineering, National I-Lan University, I-Lan 260, Taiwan, ROC

³Institute of Materials Science and Nanotechnology, Chinese Culture University, Taipei 111, Taiwan, ROC

Correspondence to: S. Lai (E-mail: smlai@niu.edu.tw)

ABSTRACT: The properties of olefin block copolymer (OBC)/thermoplastic polyurethane (TPU) blends with or without maleic anhydride (MA) modification were characterized and compared. Compared with the OBC/TPU blends, OBC-g-MA/TPU blends displayed finer morphology and reduced domain size in the dispersed phase. The crystallization temperatures of TPU decreased significantly from 155.9 °C (OBC/TPU) to 117.5 °C (OBC-g-MA/TPU) at low TPU composition in the blends, indicating the inhibition of crystallization through the sufficient interaction of modified OBC with TPU composition. The modified systems showed higher thermal stability than the unmodified systems over the investigated temperature range due to the enhanced interaction through inter-bonding. The highest improvement in tensile strength was more than fivefold for OBC-g-MA/TPU (50/50) in comparison with its unmodified blend via the enhanced interfacial interaction between OBC-g-MA and TPU. This also led to the highest Young's modulus of 77.8 ± 3.9 MPa, about twofold increase, among the investigated blend systems. A corresponding improvement on the ductility was also observed for modified blends. The modification did not vary the glass transition temperature and crystalline structure much, thus the improvement in the mechanical properties was mainly attributed to the improved compatibility and interaction from the compatibilization effect as well as increased viscosity from the crosslinking effect for modified blends. © 2016 Wiley Periodicals, Inc. *J. Appl. Polym. Sci.* **2016**, *133*, 43703.

KEYWORDS: blends; compatibilization; copolymers; polyolefins

Received 26 October 2015; accepted 27 March 2016

DOI: 10.1002/app.43703

INTRODUCTION

A polymer blending technique is an environmental friendly process due to the limited solvent hazard, so it has been an important tool to prepare novel materials and has been received much attention in the scientific and industrial community due to its cost competitive merit. Due to a growing environmental awareness, thermoplastic elastomers (TPEs) generally possess elastomeric characteristics, yet can be recycled and efficiently processed as thermoplastics unlike the encountered recycled problem for conventional rubbers. Thus, the new development of functional thermoplastic elastomers is still continuing to increase in the industry. Olefin block copolymer is a new generation of thermoplastic elastomer commercially developed by Dow Chemical. OBCs consist of crystallizable ethylene-octene blocks with high melting temperature (hard domain) at very low comonomer content, in combination with amorphous ethylene-octene blocks (soft domain) with low glass transition temperature at high comonomer content.¹ The degree of hard/soft domains could be tailored readily for various applications. Owing to these nanocrystalline hard domains, OBCs exhibit high melting tempera-

ture, but still remains soft elastomeric feature, a difficult balance hard to reach for general elastomers, like metallocene-catalyzed polyethylene elastomer. Several recent works have investigated the relationships between structure and properties of novel OBCs.^{1–5} However, only a few OBC blends available in the literature includes OBC/PP (polypropylene),^{6–9} OBC/SEBS (styrene-ethylene-butylene-styrene copolymer),¹⁰ and OBC/ethylene-octene (EO) copolymer.^{11,12}

Biodegradable polymers featuring ecological advantages have been the focus in the industry and academia as well. By incorporating bio-based polymer within the petroleum-based matrix, it would be beneficial to the environmental sustainability due to the reduced usage of petroleum-based material. Thermoplastic polyurethane (TPU) is well-known for its elasticity, oil resistance, abrasion resistance, paintability, etc.,¹³ besides its biodegradability (ester-type TPU) and recyclability. Although there were significant researches on blends of plastics and TPU, only a few works were carried out to improve the compatibility between conventional polyolefin and TPU, for instance maleic anhydride functionalized polyethylene,¹⁴ and maleic anhydride/amine functionalized

polypropylene.^{13,15} There were also only limited blends of TPE and TPU blends including polyolefin elastomer (POE)/TPU blends,¹⁶ styrene-butadiene-styrene copolymer (SBS)/TPU blends.^{17,18} To our best knowledge, no work has been done on the preparation of OBC/TPU blends. Due to the incompatibility between OBC and TPU, the blend of maleic anhydride functionalized OBC with TPU was prepared for comparison to signify the functionalized effect. In this work, at first, maleic anhydride functionalized OBC (OBC-g-MA) was prepared through a melt-blending process, and then the further addition of ester-type TPU to form OBC-g-MA/TPU blend was also prepared in the similar condition. The dispersion of TPU within the OBC matrix along with the thermal properties, tensile properties, and impact properties are elucidated in this article. Besides two compositions of OBC/TPU blends investigated at 80/20 and 50/50, we have also done some works on the evaluation of control neat resins as well. The critical composition would be another interesting topic to evaluate, especially that the authors have the experience in evaluating various contents of different compatibilizers on our other work in the past.¹⁹ This work is a representative study to demonstrate the significance of the newly developed olefin block copolymer with adjustable properties using TPU as a modifier for selective applications, such as compounding, thermoplastic elastomers, profiles, grips, etc. The mechanical properties of the blends could be tailored to meet specific applications. Hopefully, the results can be of benefit for the new polymeric systems in terms of environmental concern.

EXPERIMENTAL

Materials

The major materials used in this study were olefin block copolymer (OBC, Dow Chemical, Midland, Michigan) and thermoplastic polyurethane (TPU, Utechllan U64-DP Bayer, Leverkusen, Germany). OBC contains ethylene multiblock copolymer with the molecular weight of 123,800 g/mol and polydispersity of 3.96.²⁰ TPU is a polyester-based type with the melt viscosity of 33.2 (Pa s) at 230 °C. Maleic anhydride (MA, Acros, Morris Plains, New Jersey) was used to functionalize OBC. Dicumyl peroxide (DCP, First Chemicals, Taipei, Taiwan) was used as an initiator for grafting. Para-xylene (Acros, Thermo Fisher Scientific, New Jersey), and acetone (Acros, Morris Plains, New Jersey) were reagent grades and used as received.

Sample Preparation

For the preparation of OBC-g-MA to replace OBC as a matrix in OBC/TPU blends, the grafting reaction of MA on OBC with the addition of 0.1 or 0.2 phr (parts per hundred resins) of DCP and 1.5 phr of MA was conducted using an internal mixer (P&L Industries) under 50 rpm for 10 min at 165 °C. Then TPU was dried in the vacuum oven at 90 °C for 4 h. Modified OBC resins were dried 50 °C for 1 h. The preparation of modified OBC/TPU blends at two compositions of 80/20 and 50/50 was performed using an internal mixer above the melting temperature of TPU under 50 rpm for 5 min. The samples were hot pressed to obtain about 1 mm thin sheets.

Measurements

Grafting Percentage. The graft reaction product (4 g) was dissolved in 100 mL xylene under refluxing at 140 °C and then the hot solution

was filtered through several layers of cheesecloth. The xylene soluble product was extracted from the filtrate using 100 mL acetone. The precipitate collected and dried in a vacuum oven at 80 °C for 12 h was used to measure the grafting percentage by a titration method. The determination of the MA content was established by heating about 1 g of the sample in 100 mL of refluxing xylene at 140 °C. The solution was then titrated with 0.03N MeOH/KOH solution with phenolphthalein as an indicator. The grafting percentage was calculated.²¹

Morphological and Structure Characterizations

The functional groups were recorded on a Fourier Transform Infrared Spectrophotometer (Jasco, FT-IR-460Plus) at the resolution of 4 cm⁻¹ for 15 scans from 4000 to 450 cm⁻¹. X-ray diffraction (XRD) patterns were obtained using an X-ray diffractometer (Bruker Enraf-Nonius Kappa CCD, Bruker, Madison, Wisconsin) using CuK_α target source with a wavelength of 1.54 Å operated at 40 kV and 40 mA. The diffraction angle was scanned from 10 to 35° at a scanning rate of 2°/min. The transmission electron microscope (TEM, Hitachi H-7100 Transmission Electron Microscope, Hitachi, Hitachinaka, Ibaraki, Japan) was used to observe the dispersion status of TPU, where cryo-fractured ultrathin samples were prepared using a diamond knife without the staining process. The gel content was measured by the weight ratio of insoluble dried sample to the original sample. The samples were extracted with hot xylene and cyclohexanone to remove uncrosslinked OBC and TPU, respectively.

Thermal Analysis

Differential scanning calorimetry (DSC, DSC-4000, Perkin Elmer, Waltham, Massachusetts) was used to measure the crystallization temperature (T_c) under a cooling rate of 10 °C/min from the melting temperature after the first heating scan, and the melting temperature (T_m) at a heating rate of 20 °C/min from 30 to 250 °C in the second heating scan. The crystallinity of samples was determined from the melting enthalpy of DSC traces divided by the 100% crystalline melting enthalpy (290 J/g).^{22,23} The glass transition temperature (T_g) was determined via a dynamic mechanical analyzer (DMA, Perkin Elmer, Pyris Diamond) under a tension mode at a frequency of 1 Hz and at a heating rate of 5 °C/min from -80 to 60 °C. Thermogravimetric analysis (TGA, Pyris 1, Perkin Elmer, Waltham, Massachusetts) was used to evaluate the thermal stability of the blends under the nitrogen environment. The samples were heated from 30 to 800 °C at a heating rate of 20 °C/min.

Mechanical Test

Tensile strength, Young's modulus, and elongation at break of the samples were measured at a crosshead speed of 200 mm/min based on the ASTM-D638 standard, using a universal tensile testing machine (QC-506A1, Taichung, Taiwan). The impact test specimens were cut by a notch cutter first. The Izod impact test was performed using an impact testing machine (Gotech GT-7045).

RESULTS AND DISCUSSION

Grafting Percentage

Figure 1 shows the variations of grafting percentage at different DCP loadings with the reaction time for OBC-g-MA. It could be found that the grafting percentage of OBC-g-MA increased

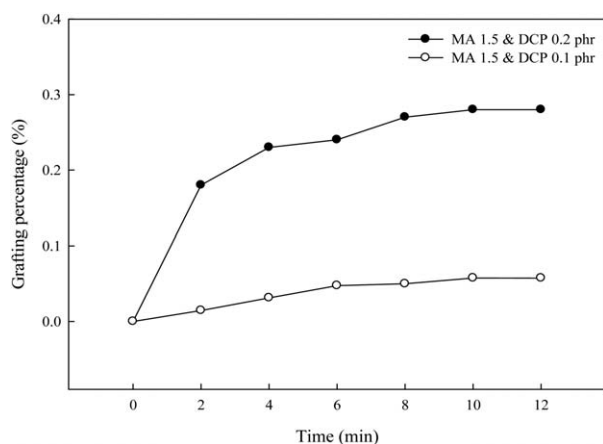


Figure 1. Variation of grafting percentage with reaction time for OBC-g-MA at different DCP loadings.

steadily with the increase of reaction time to 8 min and tended to level off afterwards. The maximum value of 0.28 wt % was in a similar order as that of metallocene-catalyzed polyethylene in our other work,²¹ although the different molecular structures were involved for two types of polyolefin. The result indicated a successful grafting process for neat OBC resin. Hereafter, the 0.2 phr peroxide-prepared OBC-g-MA was used for further investigation.

Spectroscopy Characterization

To confirm the graft reaction of maleic anhydride (MA) onto OBC, FTIR spectroscopy was used to observe characteristic peaks of maleic anhydride. Figure 2 shows the FTIR characteristic spectra of OBC and OBC-g-MA, respectively. The grafted MA was revealed through the observation of characteristic peaks at 1714, 1791, and 1866 cm^{-1} as shown in Figure 2(a), which was also manifested in the literature for other polyolefins with MA modification.^{24,25} These results indicated the successful grafting of maleic anhydride onto OBC. As for the blends, the blending of OBC/TPU with or without modification did not show clear difference due to the limited grafting moiety on the modified OBC, except the presence of anhydride group (1791 cm^{-1}) in both compositions of 80/20 and 50/50. No visible peak shift was observed to reveal the specific interaction between anhydride group on OBC-g-MA and urethane group on TPU. However, the hydrogen bonding would still be expected in comparison with that between unmodified OBC and TPU. The later discussion on the morphology observation still provides the improved compatibility for modified OBC and TPU.

Transmission Electron Microscope (TEM)

Figure 3 shows the distinct morphology for unmodified (OBC/TPU) and modified (OBC-g-MA/TPU) blends at specific compositions of 80/20 and 50/50 based on the TEM observations, respectively. The figure showed the morphology of TPU particles dispersed in the OBC matrix, which would relate two important aspects of domain size and interfacial adhesion on the mechanical properties. Interestingly, TPU and OBC-g-MA tended to form a co-continuous phase at 50/50 composition in

Figure 3(f). Compared with the OBC/TPU blends, OBC-g-MA/TPU blends displayed significantly finer morphology and reduced particle size in the dispersed phase. This was attributed to the specific interaction from maleic anhydride on OBC-g-MA and urethane group on TPU,²⁶ which even led to a formation of unusual elongated dispersed phase. This type of elongated morphology was often observed in the melt drawing process,²⁷ but not common for this simple melt mixing process unless a careful selection of process conditions and polymer systems.²⁸ Plattner *et al.*²⁹ reported an important interface stabilization mechanism to explain the observed elongated structure for polycaprolactone dispersed in the polypropylene matrix. With reduced interfacial tension, the large deformation in causing the breakup of dispersed phase became more feasible. In the end, the smaller dispersed phase was attained. In some cases, the reduction of interfacial interaction was not significant, but still in a sufficient degree, then the elongated structure was obtained. Without the interface stabilization, the dispersed domains were kind of large. In this study, our observation in the elongated structure for the modified blends was essentially justified by a certain degree of improved interfacial interaction, and the increased viscosity from the rheological concern discussed in the mechanical properties section later.

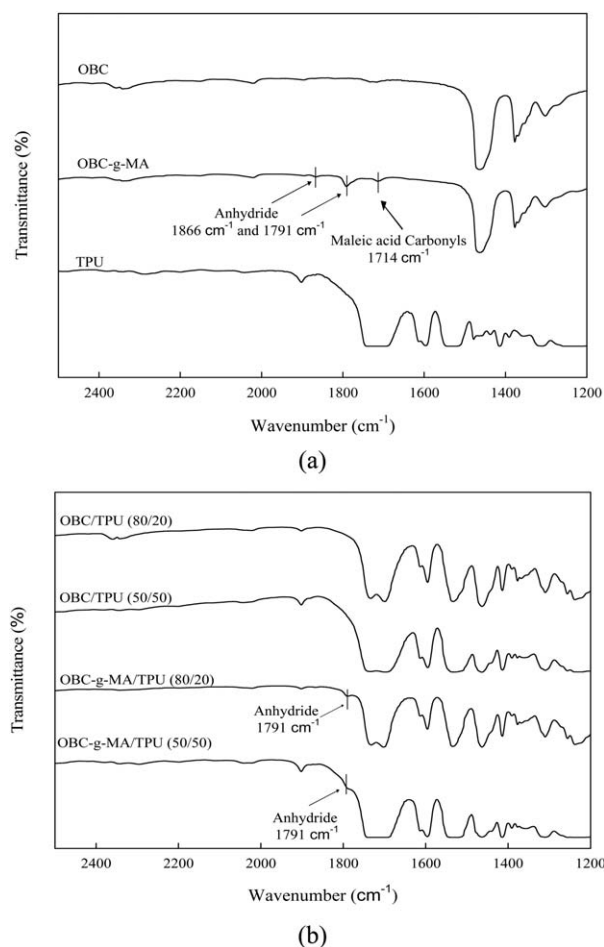


Figure 2. FT-IR spectra of (a) OBC, OBC-g-MA, and TPU, (b) OBC/TPU, and OBC-g-MA/TPU blends (1200–2500 cm^{-1}).

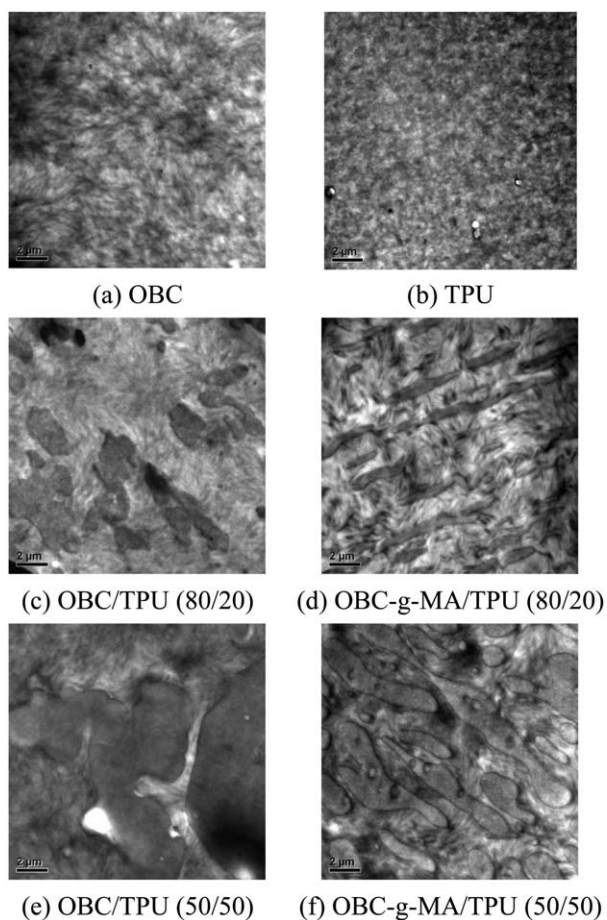


Figure 3. TEM images of OBC/TPU and OBC-g-MA/TPU at magnification of 5k (scale bar: 2 μm).

X-ray Diffraction Patterns

Figure 4 shows the XRD patterns of neat OBC, TPU, their blends with or without modification. For OBC, the characteristic diffraction peaks at 2θ of 21.5°, 23.8°, and 28.7° corresponding to (110), (200), and (210) were assigned to the crystallographic planes of the orthorhombic unit cell of polyethylene in accompanying with the broad amorphous halo centered at 2θ of 19.1°. Further modifications through maleic anhydride did not vary the crystalline structure much. The diffraction pattern of TPU showed two small diffraction peaks at $2\theta = 19.4^\circ$ and 23.8° with a small amorphous halo at 2θ of 18.2°. These peaks were attributed to the reflections on the crystal planes (110) and (200), respectively.³² The representative blend at a composition of 50/50 was chosen as a comparison. Additional tiny peak near 18.2° contributed from TPU was found for the OBC/TPU blend with respect to neat OBC. In addition, all blends with or without modification displayed similar diffraction patterns, indicating that the modification did not cause a visible change in the crystalline structure. The current result was in close agreement with the later discussion on the DSC analysis. Thus, the mechanical properties discussed later should be attributed the modification effect rather than the variation of crystalline structure.

Nonisothermal Crystallization and Melting Behaviors

The nonisothermal crystallization and melting behaviors were recorded at a cooling rate of 10 °C/min and heating rate of

20 °C/min, respectively. A comparison on OBC/TPU and OBC-g-MA/TPU blends at a typical weight ratio of 50/50 was illustrated in Figure 5. The results for other samples are shown in Table I. At a cooling rate of 10 °C/min, the values of crystallization peak temperatures (T_c , temperature at the exotherm minimum) of OBC and TPU were about 102.9 and 155.7 °C, respectively. No much variation for the crystallization temperatures for OBC in the OBC/TPU and modified OBC/TPU blends because of the relatively fast crystallization rate for its simple olefin structure. At high TPU composition of 50%, this inhibition of crystallization rate was not much, leading to a few degrees of depression in the crystallization temperatures for modified blends with respect to unmodified blends. On the other hand, the crystallization temperatures of TPU decreased significantly from 155.9 °C (OBC/TPU) to 117.5 °C (OBC-g-MA/TPU) at low TPU composition in the blends, indicating the inhibition of crystallization through the sufficient interaction of modified OBC with TPU composition. Apparently, the effect of OBC modification played an important role in the crystallization behaviors. Note that the crystallinity of modified blends was in general slightly lower than that of neat blend due to the hindrance of chain mobility from the modified effect. However, strictly speaking, the difference was quite limited and the detail

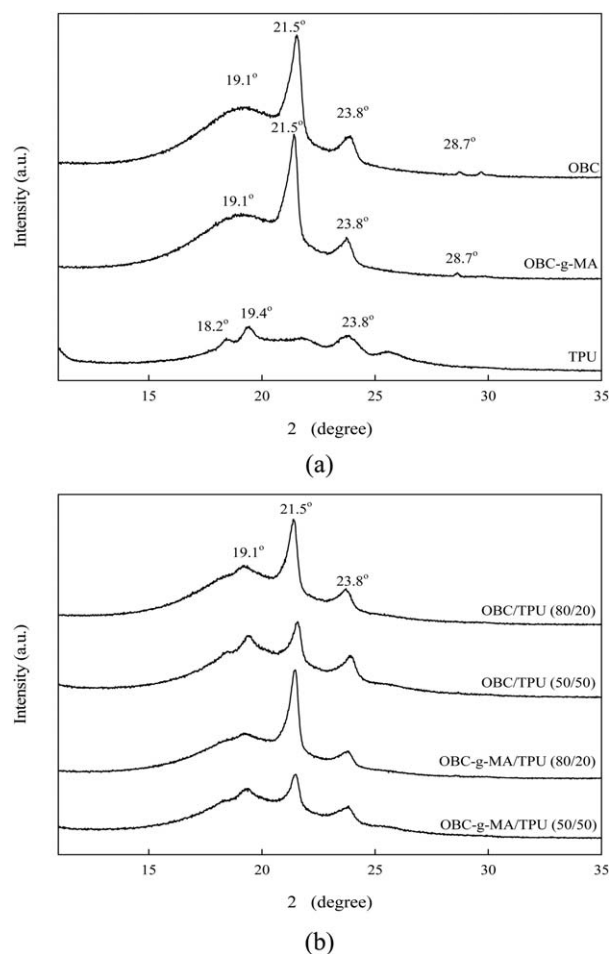
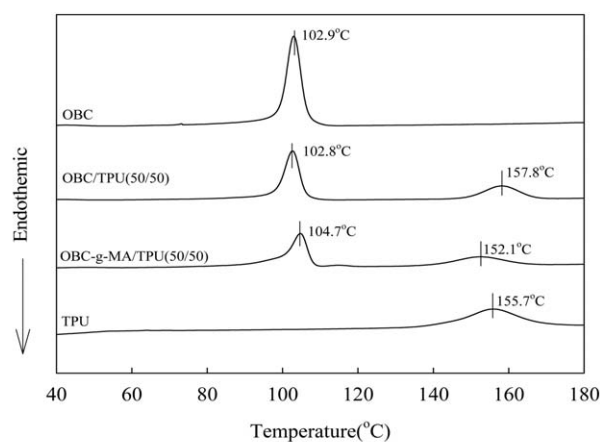
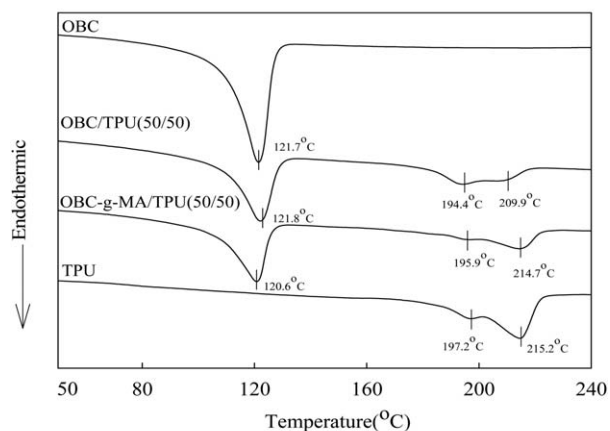


Figure 4. XRD patterns of neat resins, OBC/TPU, and OBC-g-MA/TPU blends.



(a)



(b)

Figure 5. DSC thermograms of OBC/TPU and OBC-g-MA/TPU blends (50/50), (a) cooling curves and (b) heating curves.

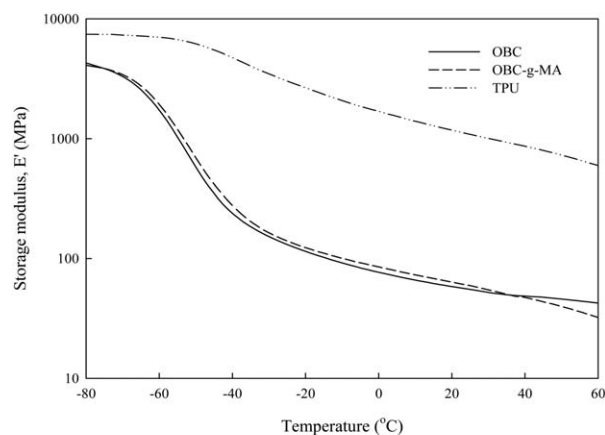
comparison was not made here because of broad peaks involved for all samples in considering the experimental errors.³³

To investigate the melting behaviors of those crystallized samples for OBC/TPU blends and modified blends, the results are also shown Table I. For a typical weight ratio of 50/50, the

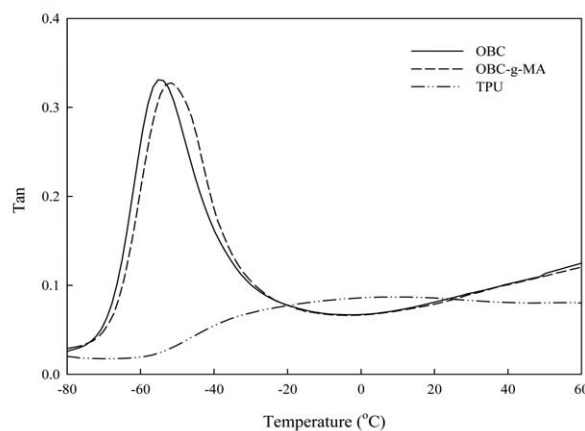
Table I. Crystallization and Melting Temperatures of OBC/TPU and OBC-g-MA/TPU Blends

Sample code	T_c , OBC	T_c , TPU	T_m , OBC	T_m , TPU
OBC	102.9	-	121.7	-
OBC/TPU (80/20)	103.2	155.9	121.7	-
OBC/TPU (50/50)	102.8	157.8	121.8	194.4, 209.9
TPU	-	155.7	-	197.2, 215.2
OBC-g-MA	102.7	-	121.3	-
OBC-g-MA/TPU (80/20)	104.4	117.5	120.6	-
OBC-g-MA/TPU (50/50)	104.7	152.1	120.6	195.9, 214.7

T_c , OBC, T_c , TPU: crystallization temperatures of OBC and TPU, respectively. T_m , OBC, T_m , TPU: melting temperatures of OBC and TPU, respectively.



(a)



(b)

Figure 6. DMA curves of OBC, OBC-g-MA, and TPU (a) storage modulus (E'), (b) $\tan \delta$.

results are shown in Figure 5(b). As discussed earlier, owing to the limited difference of the crystallinity in considering the experimental error, the melting temperatures of respective resins in all blends remained largely unchanged, suggesting that the crystal structure formation was not varied with or without the modification. The results were in agreement with the XRD investigation discussed earlier.

Dynamic Mechanical Properties

Dynamical mechanical properties were carried out to investigate the viscoelastic behaviors and glass transition temperatures of OBC/TPU blends with or without modification. The glass transition temperatures of neat OBC, OBC-g-MA, TPU, were observed in Figure 6. As for the blends, the results of OBC/TPU and modified OBC/TPU blends are shown in Figure 7. The representative dynamic storage moduli are listed in Table II. Owing to the soft nature of OBC resin, its storage modulus was considerably smaller than that of TPU. The storage modulus of OBC was similar to that of modified OBC as well. The glass transition temperature of OBC at -54.9°C was kind of lower than that of TPU at 11.1°C , but was similar to that of modified OBC resin at -52.1°C . All resins behaved general viscoelastic materials with reduced modulus against test temperature. For the blend composition at OBC/TPU (80/20) with or without

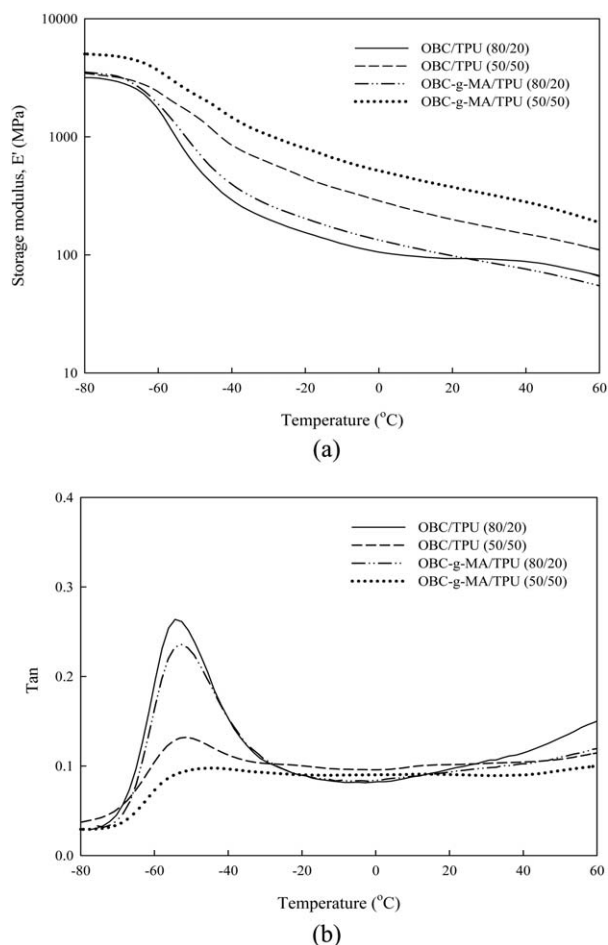


Figure 7. DMA curves of OBC/TPU and OBC-g-MA/TPU (a) storage modulus (E'), (b) $\tan \delta$.

modification, a measurable increase of storage modulus for OBC containing TPU was observed due to the reinforcing effect of TPU. A small improvement for modified blend in comparison with unmodified blend was observed. In addition, the modification did not vary the glass transition temperature much. On the other hand, for the blend composition at OBC/TPU (50/50) with or without modification, a considerable increase of storage modulus for OBC containing TPU was observed due to the increased amount of TPU. It appeared that OBC-g-MA/TPU blend conferred the further increase in the storage modulus in comparison

with OBC/TPU blend. This is attributed to highly incompatible blend of OBC and TPU without modification, as evidenced by the morphology discussed earlier. With the specific interaction between OBC-g-MA and TPU, the storage modulus increased by ca. twofold. In addition, a small shift of the glass transition temperature of OBC component toward high temperature in the OBC-g-MA/TPU blend was observed, which also suggested an increased interaction for the modified blends. Note that, even though the variation of glass transition temperatures was quite limited, the improvement in the interfacial interaction through the observation of morphology was quite evident.

Thermal Stability

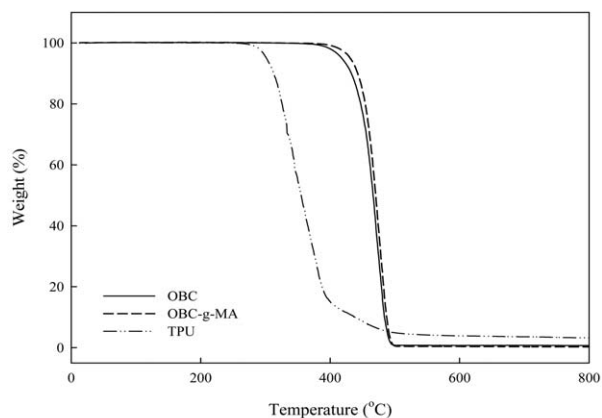
Thermogravimetric analysis (TGA) was carried out to investigate the thermal stability of the unmodified and modified systems. Figure 8 shows the thermal scans of neat resins, OBC/TPU, and OBC-g-MA/TPU blends. OBC gave higher thermal stability than TPU. The increased thermal stability for maleic anhydride functionalized OBC was also observed. Taking 5 wt % loss as an example for an index of thermal stability, Figure 8 and Table III show that the degradation temperature increased from 336.8 °C in the OBC/TPU (80/20) to 363.8 °C in the OBC-g-MA/TPU (80/20). A slightly small improvement was also found for the blend composition of 50/50 in this range due to higher amount of TPU to discount the positive contribution from the increased interaction and the use of functionalized OBC-g-MA with higher thermal stability. For the higher degradation temperatures at weight loss of 50%, the higher thermal stability was also envisaged for OBC-g-MA/TPU blend (80/20), but less improvement for blend composition of 50/50 due to the aforementioned rationale. In general, the modified systems showed higher thermal stability than the unmodified systems over the investigated temperature range due to the enhanced interaction through interbonding³⁴ in light of the usage of functionalized OBC.

Mechanical Properties

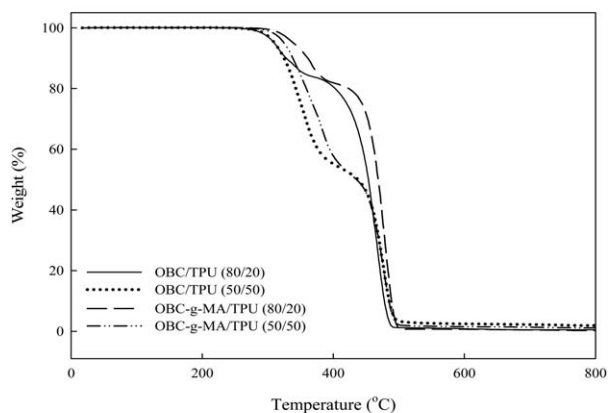
The effects of modification on tensile strength, Young's modulus, and elongation at break of OBC/TPU blends are shown in Figure 9. Owing to the soft elastomeric nature of OBC, its tensile strength was considerably smaller than that of TPU. As for functionalized OBC, tensile strength was slightly higher than that of OBC. Thus, it is advantageous to add TPU into the OBC matrix to enhance its mechanical properties. However, owing to the incompatibility between OBC and TPU, the lowest tensile strength was observed at the composition of 50/50, the

Table II. Dynamic Mechanical Analysis of OBC/TPU and OBC-g-MA/TPU Blends

Sample code	Storage modulus at 25 °C E' (MPa)	Glass transition temperature of OBC (°C)	Glass transition temperature of TPU (°C)
OBC	55.2	-54.9	-
OBC/TPU (80/20)	91.1	-53.6	11.3
OBC/TPU(50/50)	184.8	-52.8	12.7
TPU	1080.7	-	11.1
OBC-g-MA	59.5	-52.1	-
OBC-g-MA/TPU (80/20)	91.3	-52.9	10.7
OBC-g-MA/TPU (50/50)	351.7	-49.8	11.5



(a)



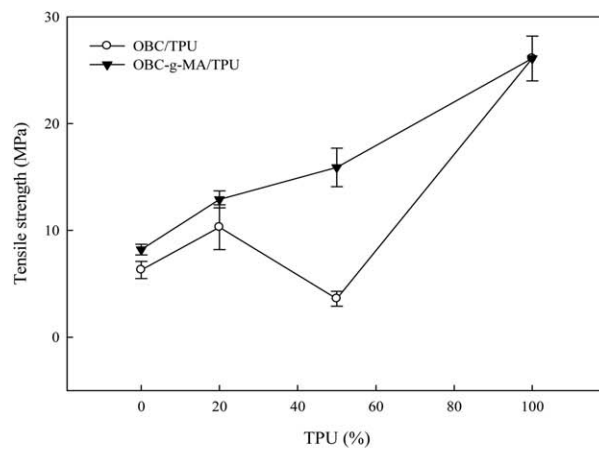
(b)

Figure 8. TGA curves of (a) neat resins, (b) OBC/TPU and OBC-g-MA/TPU blends.

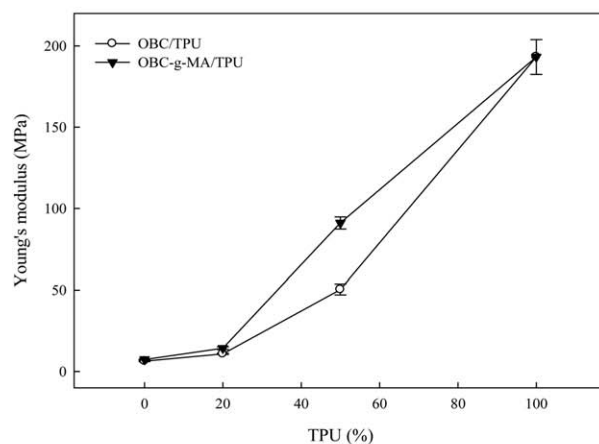
value of which was even lower than that of OBC. With maleic anhydride modification, tensile strength increased at all compositions with respect to the pure blends, which was attributed to the enhanced interfacial interaction as evidenced in TEM analyses. The highest improvement was more than fivefold for OBC-g-MA/TPU (50/50) in comparison with its unmodified blend.

Table III. Thermal Degradation Temperatures of OBC/TPU and OBC-g-MA/TPU Blends

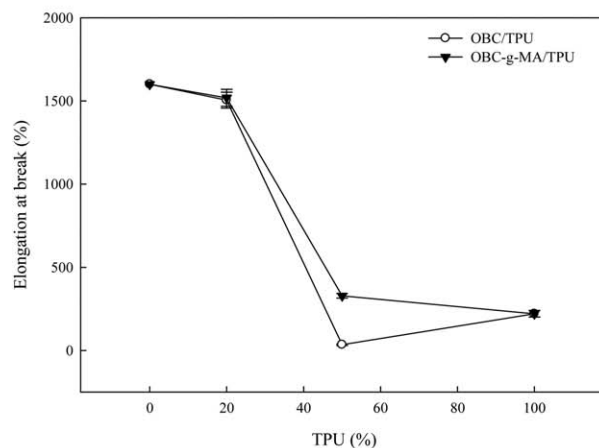
Sample code	Temperature of 5 wt % weight loss (°C)	Temperature of 50 wt % weight loss (°C)	Ash content (%)
OBC	442.9	491.8	0.4
OBC/TPU (80/20)	336.8	480.1	0.5
OBC/TPU (50/50)	335.2	462.9	1.9
TPU	331.7	384.7	3.3
OBC-g-MA	456.6	498.9	0.3
OBC-g-MA/TPU (80/20)	363.8	494.8	0.3
OBC-g-MA/TPU (50/50)	349.1	461.5	1.1



(a)



(b)



(c)

Figure 9. (a) Tensile strength, (b) Young's modulus, (c) elongation at break of OBC/TPU and OBC-g-MA/TPU blends.

To further elucidate the tensile properties, Young's modulus of OBC/TPU blends with or without modification is illustrated in Figure 9(b). Young's modulus of OBC was still in the lowest ranking among all neat or functionalized resins. Young's modulus increased with increasing TPU composition due to the rigid

Table IV. Equilibrium Torques and Gel Contents of OBC/TPU and OBC-g-MA/TPU Blends

Sample code	Torque (Nm)	Gel content (%)
OBC	11	1.3
OBC/TPU (80/20)	5	2.3
OBC/TPU (50/50)	1	3.5
TPU	-	2.3
OBC-g-MA	24	75.0
OBC-g-MA/TPU (80/20)	10	67.7
OBC-g-MA/TPU (50/50)	7	31.6

Note: The torque of TPU is virtually zero.

nature of TPU. Young's modulus of neat OBC/TPU blends was about 35.7 ± 2.3 MPa at the composition of 50/50. With the maleic modification, Young's modulus increased significantly due to aforementioned enhanced interfacial interaction between OBC-g-MA and TPU, which led to the highest Young's modulus of 77.8 ± 3.9 MPa, about twofold increase, among the investigated blend systems. Apparently, the additional modification essentially contributed to the enhanced stiffness of the prepared blends.

Besides tensile strength and Young's modulus, elongation at break was included for better demonstrating the improved mechanical properties after the grafting process, as shown in Figure 9(c). Owing to the soft elastomeric nature of OBC, its elongation at break was considerably larger than that of TPU. As for functionalized OBC, elongation at break resembled to that of OBC. Elongation at break decreased with increasing TPU composition due to the rigid nature of TPU. The lowest elongation at break of neat OBC/TPU blends was about $34.3 \pm 2.5\%$ at the composition of 50/50. With the maleic anhydride modification, elongation at break increased to $328.2 \pm 13.9\%$, almost tenfold increase, due to the aforementioned enhanced interfacial interaction between OBC-g-MA and TPU. This corresponded to the largest increment among the investigated blend systems. Apparently, the additional modification essentially contributed to the enhanced ductility of the prepared blends.

Besides the tensile properties, the impact property was also reported here. The impact strength could not be attained for OBC, OBC-g-MA, OBC/TPU (80/20), OBC-g-MA/TPU (80/20), OBC-g-MA/TPU (50/50), and TPU due to elastomer characteristics of both OBC and TPU without failure under the impact testing. On the other hand, the impact strength of OBC/TPU (50/50) was determined to be about 106.9 ± 8.8 (J/m). This result indicated the higher impact strength for the modified blend of 50/50 composition.

Overall, these mechanical properties justified the performance of the modified blends, attributing to the improved dispersion of TPU in the modified blends as seen in TEM morphology. During the grafting and mixing process, we also noted the microgel formation from the inevitable peroxide crosslinking effect, besides the peroxide-initiated grafting process. Table IV lists the gel contents of all samples including control samples prepared at the mixing temperature. The insoluble gel content was about 75.0% for OBC-g-MA, which was significantly higher

than that of OBC and TPU at 1.3 and 2.3%, respectively. This microgel formation might be attributed to the inevitable peroxide crosslinking effect, besides the peroxide-initiated grafting process. Owing to the improved compatibility and interaction from the compatibilization effect as well as increased viscosity from the crosslinking effect during mixing process, the corresponding gel contents of OBC-g-MA/TPU (80/20) and (50/50) were at 67.7 and 31.6%, which were significantly higher than those of OBC/TPU (80/20) and (50/50) at 2.3 and 3.5%, respectively. Although these microgels dispersed in the blends might deteriorate the properties of modified blends, yet the properties were still improved, especially for 50/50 composition. Note that the mechanical properties of OBC-g-MA resembled to those of OBC, thus the increased mechanical properties for the modified blends were mainly attributed to the good dispersion of TPU domains.

From the TEM morphology, the big dispersed domains were transformed to small dispersed domains, especially for OBC-g-MA/TPU blend at 50/50 composition. In addition to the compatibilization effect, the rheology factor is also an important factor to consider for the improved TPU dispersion to enhance mechanical properties. As the grafting process produced insoluble gels and the plunger forces exceeded the limitation of the TA AR2000 instrument for OBC-g-MA/TPU blends during testing, thus the viscosity values could not be determined in these shear rate ranges. This phenomenon of increased crosslinking or entanglement through the formation of interchain chemical bonds for POE-g-MA/TPU blends was also addressed, which in turn increased the melt viscosity.²⁶ However, by closely monitoring the mixing process, the melting torques during mixing in the internal mixer could be recorded as an index of melt viscosity.³⁵ As shown in Table IV, the equilibrium torques of TPU, OBC, and OBC-g-MA were virtually zero, 11, and 24 Nm, respectively. Owing to the improved compatibility and interaction as well as increased viscosity from the crosslinking effect during mixing process, the equilibrium torque of OBC-g-MA/TPU (80/20) at 10 Nm was higher than that of OBC/TPU (80/20) at 5 Nm. In addition, the torque value increased up to sevenfold for OBC-g-MA/TPU (50/50) at 7 Nm in comparison with OBC/TPU (50/50) at 1 Nm. This torque variation was evidently larger than that of OBC-g-MA relative to OBC, suggesting an improved specific interaction between OBC-g-MA and TPU. Thus, the increased compatibility due to the decreased interfacial tension and the increased viscosity tended to promote the dispersion of dispersed TPU domains, which dominated the negative contribution from the insoluble gels. Note that the modification did not cause a visible change in the crystalline structure as described in the DSC and XRD analyses, thus the main contribution from the maleic anhydride modification was justified. In general, the improved interfacial interaction between OBC-g-MA and TPU did confer the observable difference in mechanical properties, especially for the composition of 50/50.

ACKNOWLEDGMENTS

The authors are grateful to Ms. Yun-Lan Chu and Mr. Yen Ju Chen for helping manuscript preparation.

CONCLUSIONS

The properties of olefin block copolymer (OBC)/thermoplastic polyurethane (TPU) blends with or without maleic anhydride (MA) modification were characterized. Compared with the OBC/TPU blends, OBC-g-MA/TPU blends displayed finer morphology and reduced domain size in the dispersed phase. The crystallization temperatures of OBC did not vary much, but those of TPU decreased in the modified blends, indicating the inhibition of crystallization through the sufficient interaction of modified OBC with TPU composition. The modified systems showed higher thermal stability than the unmodified systems over the investigated temperature range due to the enhanced interaction through inter-bonding. Tensile strength increased at all compositions with respect to the pure blends. The highest improvement in tensile strength was more than fivefold for OBC-g-MA/TPU (50/50) in comparison with its unmodified blend via the enhanced interfacial interaction between OBC-g-MA and TPU. Additional improvement in Young's modulus and ductility was observed as well. The modification did not vary the glass transition temperature and crystalline structure much; thus, the improvement in the mechanical properties was mainly attributed to the improved compatibility and interaction from the compatibilization effect as well as increased viscosity from the crosslinking effect for modified blends. The specific interaction was essential to the properties enhancement of derived OBC/TPU blends.

REFERENCES

1. Wang, H.; Taha, A.; Chum, S. P.; Hiltner, A.; Baer, E. *ANTEC* **2007**, 2, 1181.
2. Lin, Y.; Marchand, G. R.; Hiltner, A.; Baer, E. *Polymer* **2011**, 52, 1635.
3. Lin, Y.; Yakovleva, V.; Chen, H.; Hiltner, A.; Baer, E. *J. Appl. Polym. Sci.* **2009**, 113, 1945.
4. Wu, S.; Wu, J.; Huang, G.; Li, H. *Macromol. Res.* **2015**, 23, 537.
5. Wen, T.; Zhou, Y.; Liu, G.; Wang, F.; Zhang, X.; Wang, D.; Chen, H.; Walton, K.; Marchand, G.; Loos, J. *Polymer* **2012**, 53, 529.
6. Ares, A.; Pardo, S. G.; Abad, M. J.; Cano, J.; Barral, L. *Rheol. Acta* **2010**, 49, 607.
7. Jin, J.; Zhao, C.; Du, J.; Han, C. C. *Macromolecules* **2011**, 44, 4326.
8. Liu, G.; Zhang, X.; Li, X.; Chen, H.; Walton, K.; Wang, D. *J. Appl. Polym. Sci.* **2012**, 125, 666.
9. Li, Z.; Shi, Y. J.; Sun, C. X.; Zhang, Q.; Fu, Q. *Compos. Sci. Technol.* **2015**, 115, 34.
10. Poon, B.; Ansems, P.; Weinhold, J.; Marchand, G. *ANTEC* **2008**, 2, 762.
11. Khariwala, D. U.; Wang, H. P.; Weinhold, J.; Chen, H.; Hiltner, A.; Baer, E. *ANTEC* **2008**, 1, 114.
12. Raja, P. R.; Wilson, J. K.; Peters, M. A.; Croll, S. G. *J. Appl. Polym. Sci.* **2013**, 130, 2624.
13. Lu, Q. W.; Macosko, C. W. *Polym. Mater. Sci. Eng.* **2003**, 89, 844.
14. Di, Y.; Kang, M.; Zhao, Y.; Yan, S.; Wang, X. *J. Appl. Polym. Sci.* **2006**, 99, 875.
15. Lu, Q. W.; Macosko, C. W.; Horriion, J. *J. Polym. Sci. A: Polym. Chem.* **2005**, 43, 4217.
16. Wang, J. S.; Chen, X. D.; Mai, B. Y.; Zhang, M. Q.; Rong, M. Z. *J. Appl. Polym. Sci.* **2007**, 105, 1309.
17. Wu, J. H.; Li, C. H.; Chiu, H. T.; Shong, Z. J.; Tsai, P. A. *Polym. Adv. Technol.* **2010**, 21, 164.
18. Wu, J. H.; Li, C. H.; Wu, Y. T.; Leu, M. T.; Tsai, Y. *Compos. Sci. Technol.* **2010**, 70, 1258.
19. Lai, S. M.; Chen, C. M. *Eur. Polym. J.* **2007**, 43, 2254.
20. Hustad, P. D.; Szuromi, E.; Timmers, F. J.; Carnahan, E. M.; Clark, T. P.; Roof, G. R.; Klamo, S. B.; Arriola, D. J. *Dow Global Technol.* **2012**, US20120083575 A1.
21. Wu, C. S.; Liao, H. T.; Lai, S. M. *Polym. Plast. Technol. Eng.* **2002**, 41, 645.
22. Park, H. E.; Dealy, J. M.; Marchand, G. R.; Wang, J. A.; Li, S.; Register, R. A. *Macromolecules* **2010**, 43, 6789.
23. Wang, H. P.; Chum, S. P.; Hiltner, A.; Baer, E. *J. Polym. Sci. B: Polym. Phys.* **2009**, 47, 1313.
24. Bikiaris, D. N.; Vassiliou, A.; Pavlidou, E.; Karayannidis, G. P. *Eur. Polym. J.* **2005**, 41, 1965.
25. Lai, S.; Ti, K. *Polymer* **2007**, 22, 502.
26. Yang, J.; Chen, X.; Fu, R.; Chen, H.; Wang, J. *J. Appl. Polym. Sci.* **2008**, 109, 3452.
27. Gonzaleznunez, R.; Favis, B. D.; Carreau, P. J.; Lavallée, C. *Polym. Eng. Sci.* **1993**, 33, 851.
28. Vacková, T.; Slouf, M.; Nevoralová, M.; Kaprálková, L. *Eur. Polym. J.* **2012**, 48, 2031.
29. Plattier, J.; Benyahia, L.; Dorget, M.; Niepceron, F.; Tassin, J. F. *Polymer* **2015**, 59, 260.
30. Kavesh, S.; Schultz, J. M. *J. Polym. Sci. Polym. Phys.* **1970**, 8, 243.
31. Chiu, F. C.; Lai, S. M.; Ti, K. T. *Polym. Test.* **2009**, 28, 243.
32. Čulin, J.; Šmit, I.; Vekšli, Z.; Anžlovar, A.; Žigon, M. *Polym. Int.* **2006**, 55, 285.
33. Lai, S. M.; Li, H. C.; Liao, Y. C. *Eur. Polym. J.* **2007**, 43, 1660.
34. Chiu, F. C.; Lai, S. M.; Li, H. C.; Chen, C. C. *J. Polym. Res.* **2011**, 18, 627.
35. Lai, S. M.; Hung, K. C.; Lai, W.-J.; Zeng, J.-W.; Cheng, K. C. *J. Appl. Polym. Sci.* **2014**, 131, DOI: 10.1002/app.40830.